Effects of Engine Loads on Exhaust Emissions and Particulate Matter with Morphological Characteristics in a Common Rail 4 Cylinder Diesel Engine

Hyun Gu Roh[*] · Seuk Cheun Choi[**] · Chang Sik Lee[***†]

ABSTRACT

The purpose of this paper is to investigate the effects of fuel injection strategy and engine load on the structure and emissions characteristics of a DI diesel engine with 1.6L of piston displacement. In order to analyze the particulate matter (PM) and exhaust emissions characteristics in a direct injection diesel engine, the quantity of PM and exhaust emissions (including HC, CO and NO_X) were investigated under various injection strategies and engine loads. Two different injection strategies (one pilot/main injection and two pilots/main injection) was investigated under the various engine loads. A thermophoretic sampling method with a scanning electron microscope (SEM) were used to obtain the PM morphology (including primary particles, the size of the agglomerates, the number of agglomerates, the fractal dimension). The quantity of soot gradually increased with increasing engine load at both injection strategies. The primary particles in the PM agglomerates indicate that the average of the primary particle and radius of gyration increased as the engine load increased.

Key Words : Diesel engine, Engine load, Injection strategy, PM morphology and Injection strategy

---
Nomenclature

Alphabets

A_a	: Projected area
$ATDC$	: After top dead center
$BTDC$	: Before top dead center
CO	: Carbon monoxide
D_f	: Fractal dimension
d_P	: Primary particle size
H	: Height of projected area
HRR	: Rate of heat release
P_{inj}	: Injection pressure
L	: Maximum length of projected area
τ_{main}	: Main injection timing

NO_X	: Nitrogen oxide
N_P	: Number of primary particles in agglomerate
P	: Combustion pressure
τ_{p1}	: First pilot injection timing
m_{p1}	: First pilot injection quantity
τ_{p2}	: Second pilot injection timing
m_{p2}	: Second pilot injection quantity
PM	: Particulate matter
R_g	: Radius of gyration
TDC	: Top dead center
$ULSD$	: Ultra low sulfur diesel

1. Introduction

Diesel engines are widely used for a variety of power generation needs in industrial production, commercial and military applications. In these usage, diesel combustion for a compression ignition engine produces signi-ficantly more particulate matter (PM) than gasoline fueled combustion[1]. Diesel engine combustion produces unexpected products such as PM and emission gases including carbon monoxide (CO), hydrocarbon (HC) and nitrogen oxide (NOx). The PM and emission gases from diesel engines may cause health (e.g., emphysema and dizziness) and environmental problems. It is well known that small sized PM (commonly refer as nano particles or soot) are serious contaminants in the human respiratory system[2].

In 1996, the EPA reported that emissions from land-based nonroad, marine, and diesel engines were the

* Induk, University, Department of Mechanical & Automobile Engineering

** Korea Instititute of Industrial Technology, Korea National Cleaner Production Center, Green Management Planning Office

*** Hanyang, University, Department of Mechanical Engineering

† 연락저자, cslee@hanyang.ac.kr

main causes of PM_{10} (PM less than 10 microns in diameter), which was estimated to be about 40 percent of the total mobile sources[3]. Additionally, the EPA began a new program to help the Clean Air Act's goal of cleaning up the nation's air by reducing emissions from the nonroad sector. This program began to see significant reductions in emissions in 2008, and by 2030 estimate that it will reduce the amount of $PM_{2.5}$ (PM less than 2.5 microns in diameter) by 129,000 tons annually. This final rules set emission standards for nonroad diesel engines that will achieve reductions in $PM_{2.5}$ emissions levels in excess of 95%[3,4]. Therefore, the reduction of diesel PM has become a major focus for experimental and numerical analysis in the combustion community due to the restrictive air pollution regulations imposed by various governmental and environmental agencies. Researchers generally use a smoke meter with a light extinction method to measure quantity of PM. This method is commonly used for emission measurements of diesel PM as it is suitable for the measurement of heavy, sooty combustion emission. In general, the sensing volume for the measurement of PM by extinction must contain a large particle concentration. Total extinction is the sum of the absorption and the scattering extinction and can be a function of both particle composition and size[5,6]. However, the smoke meter method has its disadvantages, including a low sensing volume for small particle concentrations, and it may not provide PM morphological properties. Therefore, the measurement of PM with this method may not accurately reflect the accurate volume of PM mass or morphological properties.

To overcome these disadvantages, the combination of these measurements with a PM morphology measurement technique (commonly referred to as a thermophoretic sampling technique) is suggested. In an effort to accurately measure nano particles, PM morphology measurements (i.e. the size of primary particles, agglomerate size, and fractal dimension) require investigation of the PM formation of diesel engine systems. PM morphology gives additional information to aid in the understanding of soot formation mechanisms [7,8].

In previous studies, PM morphology measurements were obtained using a diesel engine with a thermophoretic sampling technique. These measurement indicate that primary particle size and agglomerate size depend on the engine operating conditions (engine

load and engine speed) and the duty of diesel engine (light or heavy duty)[8-10]. For example, Zhu et al[9] performed the primary particle size measurements for the PM of a light/heavy-duty diesel engine using a thermophoretic sampling technique. Variations in the primary particle size ranged from 19.6 nm to 32.5 nm under different engine operating conditions were observed in these study. However, most samples were obtained using a fixed injection strategy and injection timing due to the difficulty of injection control. Work performed by Kim et al[11] studied the measurement of combustion pressure and rate of heat release using a single cylinder diesel engine under two different injection strategies. They concluded that the split injection strategy caused a 25% reduction in maximum combustion pressure compared with the single injection strategy. They also found that the corresponding maximum rate of heat release for the split injection strategy was 25% lower than that for the single injection strategy. Different maximum combustion pressures and rates of heat release strongly influence the PM formation mechanism. The fine control of injection strategies is the most challenging aspect in the measurement of PM morphology. In the present studied, exhaust emissions and PM morphology were measured using fine engine control, including different injection strategies and injection timing.

The purpose of this study is to investigate the influence of three different engine loads (0%, 20% and 40%) and two different injection strategies (one pilot/main injection and two pilots/main injection) on PM morphology using a thermophoretic sampling method (with image process analysis), quantity of PM using smoke meter and emissions characteristics (CO, HC and NOx,) using an exhaust gas analyzer. Also, the engine performance and injection characteristics such as combustion pressure, rate of heat release, exhaust gas temperature and injection mass were investigated in order to compare the PM and emissions characteristics.

2. Experimental apparatus and procedure

2.1. Experimental apparatus

Fig. 1 shows a schematic diagram of the experimental system used in the present study. The experimental apparatus was composed of a diesel engine, an EC dynamometer, the engine control system, an
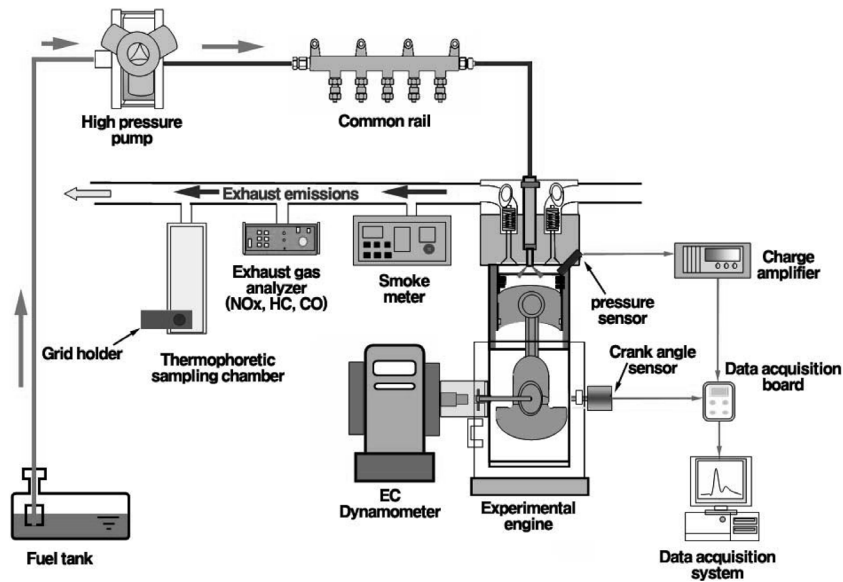
Fig. 1. Schematic of the experimental apparatus for diesel engine.

Table 1. Specifications of the test engine

Engine type	4-stroke VGT DI diesel engine
Number of cylinders	4
Bore x Stroke (mm)	77.2×84.5
Displacement volume (cm^3)	1,582
Fuel injection system	Bosch common rail
Compression ratio	17.3
Max. Power (kW/rpm)	86/4,000
Max. Torque (Nm/rpm)	260/2,000
Max. Speed (rpm)	4,750

exhaust emission gas analyzer, and a smoke meter. In this experiment, a light duty CRDI diesel engine with a displacement volume of 1,6 L and 260 Nm/2,000 rpm of maximum torque was used to analyze the PM and exhaust emissions. The specifications of the test engine are listed in Table 1.

The engine speed and load were controlled by an EC dynamometer system (Froude Consine Ltd, AG 150). The combustion and engine operating were controlled by engine control software (ETAS, INCA V5.4) and the cylinder pressure was measured using a piezoelectric type pressure sensor (Kistler, 6057ASP) with a charge amplifier (Kistler, 5011). The pressure signal and injection timing were obtained using a data acquisition board (NI, PCI 6251 snd SC2345) and data acquisition software (NI, LabVIEW V8.2). Exhaust emissions, including PM, NOx, CO and HC gas were

measured using a smoke meter (AVL, 407) and an emission gas analyzer (Horiba, MEXA-554JKNOx). In order to obtain more accurate PM morphology measurements (primary particle size and aggregate size), a thermophore the PM sampling technique was used with a thermophore the force coated electron micro copper grid (Ted Pella Inc., 01820). PM morphology images were obtained using Scanning Electron Microscope (SEM; JEOL, JSM 6701F). Measurements of primary particle and agglomerate size were taken using an image processing program (Macro script[R], Matrox Inspector 4.0).

2.2. Experimental procedures

Ultra low sulfur diesel fuel (maximum sulfur content 50 wt ppm) was used in this work. In order to investigate the effects of injection strategies on engine performance and emission characteristics, two different injection strategies were applied. The experiment was performed under a constant engine speed of 1,500 rpm, and the common rail injection pressure was kept at 50 MPa. Low engine operating load conditions (less than 50%) are commonly used to study the influence of injection timing on NOx formation[12]. In addition, a low engine operating load was selected to reduce the large variation of thermal effects on PM formation and oxidation. Three different low engine operating loads (0%, 20% and 40%) were used, as well as two different injection strategies (one pilot/main injec-

tion and two pilots/main injection). Also the pilot injection quantity was injected by 1.2 mg/stroke and main injection quantity was injected a variable according to engine load. The time of injection interval was defined as the time between the first injection and the second injection. The injection distance time is an important factor that influences engine performance and emission characteristics, and a 10° crank angle fixed value was used in the present study. With one pilot/main injection, the injection timing of the first pilot injection was started at 10° BTDC (before top dead center) and the injection timing of the main injection was started in TDC (top dead center). In the case of two pilots/main injection, the injection timing of the first pilot injection was started at 20° BTDC; the injection timing of the second pilot injection was started at 10° BTDC and the injection timing of the main injection was started in TDC. Injection timing was defined by the start of the injection signal in separate injection conditions. The injection timing is an important factor that is strongly related to engine emission gases and PM[11,13]. In order to reduce the influences of engine performance and exhaust emission, other parameters (i.e. exhaust gas recirculation; EGR, injection timing etc.) were kept constant.

During each engine experiment, three sampling tubes were directly inserted in the exhaust pipe. The exhaust gas was analyzed using a gas analyzer tube through the shuttle valve. Simultaneously, a smoke meter was used for the quantity of PM measurement and PM morphology sample was taken by sampling chamber with copper grid. The PM mass was determined as an average of readings taken every two minutes at the PM morphology conditions. The sample of PM agglomerates for studying the morphology was collected inside the thermophoretic sampling chamber. Diesel PM agglomerates were collected using an electron micro copper grid with a special TEM grid holder. SEM images were obtained using this grid with a scanning electron microscope (SEM). Two different magnifications were used: a high magnifications (100,000x) was used in the measurement of the primary particles and a low magnifications (20,000x) was used in the measurement of the size of the agglomerates. The high magnification was selected specifically for the primary particle size measurement, as it allowed for one agglomerate per image. The agglomerates for diesel PM consist of individual spherical particles that are con-

nected in a chain like structure. The size of primary particle (d_p) was measured using this magnification with randomly selected primary particles. The low magnification provided multiple agglomerates per image. The number of particles agglomerates (N_p), the radius of gyration (R_g), and the factor dimension (D_f) were determined using these low magnification SEM image. The number of particles in the agglomerates was determined by following equation with determined primary particles[14]:

$$N_p = \left[\frac{4A_a}{d_p^2 \pi} \right]^{1.09}$$

The fractal dimension based on the measured number of particles in the agglomerates is given by following equation[15]:

$$D_f \cong \frac{\log N_p}{\log(L/d_p)}$$

The size of combustion generated agglomerates (radius of gyration, Rg) was calculated by following equation using the measured factor dimension and the maximum agglomerate length[16]:

$$R_g = \left(\frac{D_f}{D_f + 2} \right)^{1/2} (L/2)$$

In order to compare the radius of gyration with commonly used values of agglomerate size, the radius of agglomerates (R) was determined from TEM images using the following equation[17]:

$$R = \frac{1}{2} \sqrt{HW}$$

3. Experimental results and discussion

In engine combustion, the exhaust emissions and PM are strongly influenced by engine operating conditions, including engine loads, engine operating speeds, injection timing and injection strategies. Previous researchers have reported that different diesel injection strategies lead to different PM morphological properties and concentrations of HC, CO and NOx[11,13].
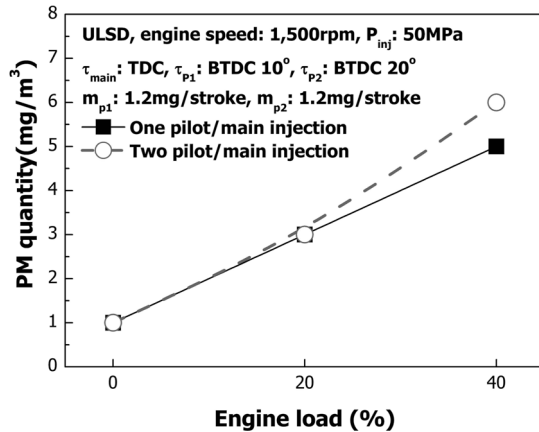
Fig. 2. Effect of the two different injection strategies on the quantity of PM for the four different engine loads.

3.1. Quantity of PM and particulate morphology

Fig. 2. show quantity of PM at three different engine operating loads for the two injection strategies. As displayed in the figure, the PM mass ranged from 1 mg/m^3 at 0% to 6 mg/m^3 at 40% for the two injection strategies. The PM mass increased three fold as the engine load was increased. The difference in PM concentration between the low engine load and the high engine load can be attributed to the influence of several PM morphological factors, including the effect of primary particle size, number of agglomerates, agglomerate size (radius of gyration or radius), and fractal dimension. In order to investigate the influence of these PM morphology factors, we used a thermophoretic sampling method to measure PM morphology.

Fig. 3(a)~(c) show the SEM images of diesel PM at three different operating engine loads (0% to 40%) for one pilot/main injection at a magnification of 100,000x. This magnification was selected specifically for the primary particle size measurements to increase the resolution of the image processing analysis. As illustrated in the PM images, the agglomerates for the three different engine loads consist of individual spherical particles (which are also referred to as the primary particles in this study). The primary particle diameter was determined from the average value of 120 PM samples obtained from the three different engine loads at the two injection strategies.

Fig. 4(a)~(c) show the distributions of the measured primary particles for the three different engine loads at one pilot/main injection. Examination of the primary particle distribution indicates the presence of larger primary particles at 40%. The primary particle at the 0% engine load shows a particle distributions in which 36% of the primary particles are greater than 20 nm, while the 40% engine load has 63% of primary particles greater than 20nm. The primary particles ranged from 19 nm at 0% to 25 nm at 40%. The primary particle size increased 125% as the engine load was increased, as shown in Table 2. Similar behaviors were observed with two pilots/main injection.

Table 2. Diesel PM morphology from thermophoretic measurements

Injection strategy	Engine load (%)	d_p (nm)	R_g (nm)	R (nm)	D_f
One pilot/main	0	19	49	52	1.47
	20	21	54	57	1.63
	40	25	71	76	1.66
Two pilots/main	0	19	51	55	1.66
	20	22	58	62	1.66
	40	26	68	73	1.71

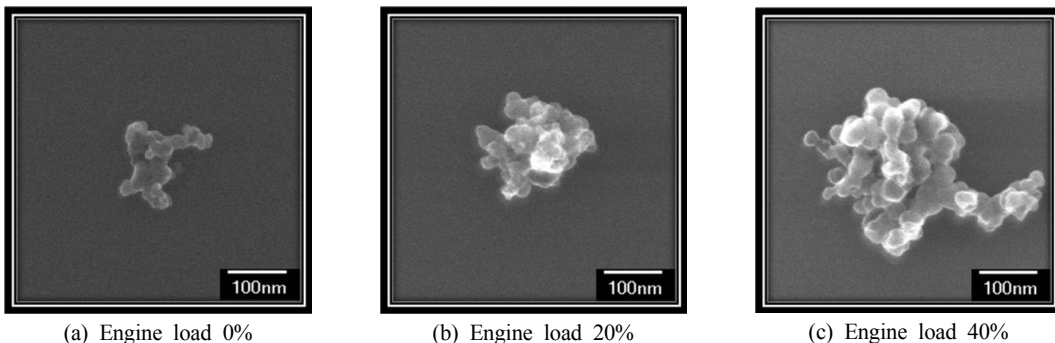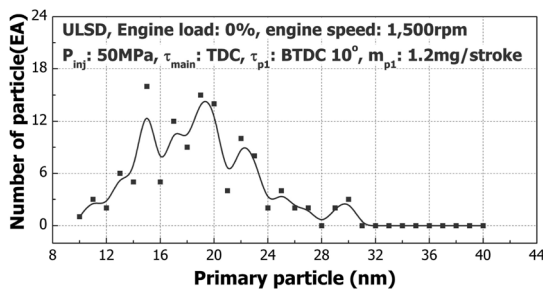(a) Engine load 0%   (b) Engine load 20%   (c) Engine load 40%

Fig. 3. SEM images for the three different engine loads with the one pilot/main injection strategy (100,000x).

The maximum primary particle was 25 nm with one pilot/main injection and 26 nm with the two injection strategy, both at the 40% engine load. The primary factors contributing to the larger size under higher loads are the stoichiometric air-fuel ratio, soot precursors (PAH species), particle nucleation and particle growth time. Considering the production of primary particles in PM emissions, the first influence factor is fuel injection mass. The injection mass increased more than 220% (proportional to the stoichiometric air fuel ratio) as the engine load increased from 0% to 40%.

Increasing injection mass with increasing engine load makes for rich air/fuel ratio conditions inside the combustion chamber, which may lead to an increasing reaction rate and result in increasing the maximum combustion pressure and exhaust temperature[11]. The increase in combustion temperature in the engine

may lead to increasing particle formation. Second, particle growth and enhancements in particle nucleation and growth are caused by soot precursors (PAH species including benzene, naphthalene and pyrene). The surface growth mechanisms through PAH addition reactions can enhance the growth of soot particles[18]. Third, particle growth at low temperatures (below combustion 400℃) is strongly influenced by particle nucleation. The combustion temperature increased according to the increase in engine operating loads. Increasing the combustion temperature may lead to increasing particle nucleation and particle growth[9]. Fourth, particle growth is strongly related to the role of precursor molecules and the time of particle growth. The high concentration of precursor molecules was produced under high engine operating
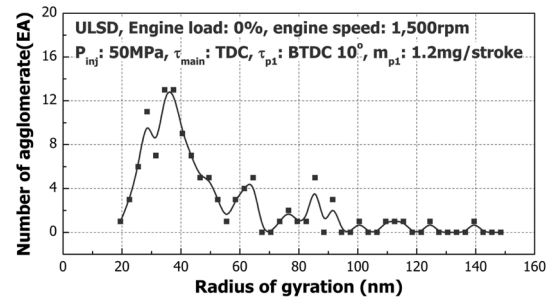

(a) 0% engine load
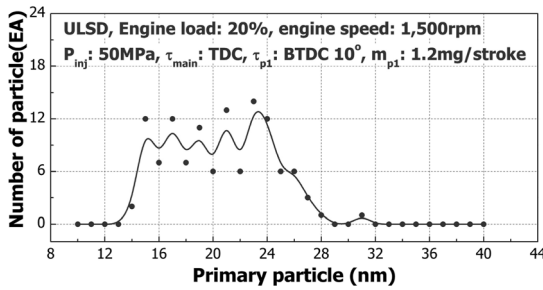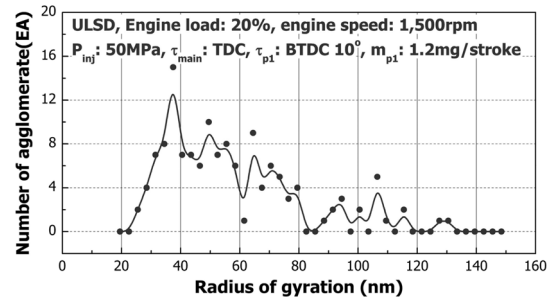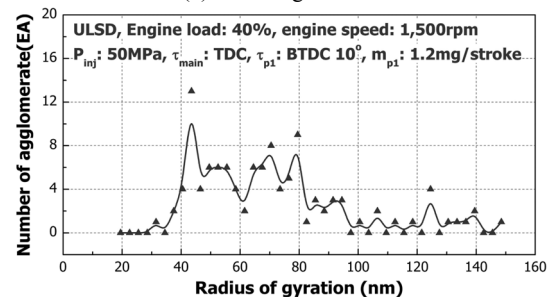

(b) 20% engine load
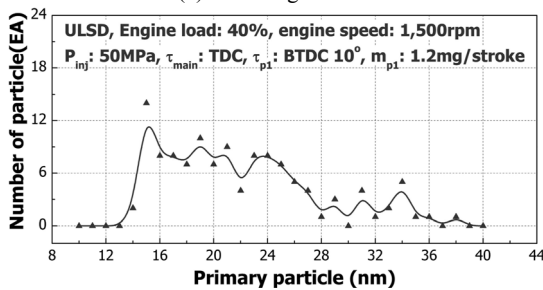
(c) 40% engine load

Fig. 4. Distributions of the primary particle at various engine loads and one pilot/main injection.

(a) 0% engine load

(b) 20% engine load

(c) 40% engine load

Fig. 5. Distributions of the radius of gyration at various engine loads and one pilot/main injection.

load conditions. The high concentration of precursor molecules leads to fast particle growth[19]. The radius of gyration was determined by using these low magnification images together with equations (1) to (3). The radius of gyration was obtained for each set of conditions by analyzing approximately 120 agglomerates.

Fig. 5(a)~(c) display the distributions of the measured radius of gyration for the three different engine loads at one pilot/main injection. This figure shows that 26% of the radius of gyration were greater than 50 nm at the 0% engine load. In the case of the 40% engine load, 61% of the radius of gyration were greater than 50 nm. The radius of gyration ranged from 49 nm at 0% to 71 nm at 40% with one pilot/main injection, as shown in Table 2 and Fig. 6. The radius of gyration ranged from 51 nm at 0% to 68 nm at 40% with two pilots/main injection. The radius of gyration increased 145% as the engine load increased from 0% to 40% with the one pilot/main injection strategy. Similar behavior was observed using two pilots/main injection. The maximum radius of gyration was 71 nm with one pilot/main injection and 68 nm with two pilots/main injection at the 40% engine operating load.

Radius for the three engine loads and two injection strategies also shown in Fig. 6. The radius of gyration was ranged from 52 nm at 0% and one pilot/main injection to 71 nm at 40% engine load and one pilot/main injection. The maximum radius increased 146% and 133% as the engine load increased for the one pilot/main injection and the two pilots/main injection strategies, respectively. There are several impor-
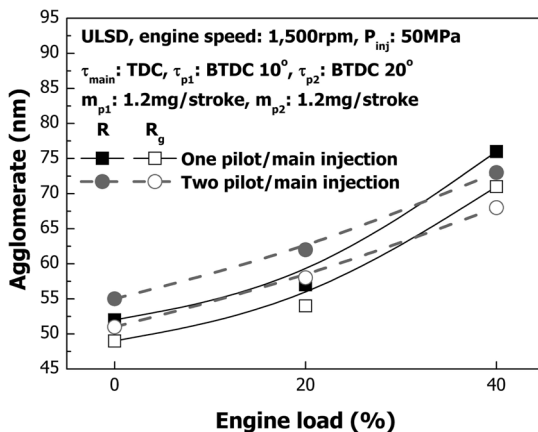
tant implications of the increase in soot agglomerate (i.e. radius of gyration) as the engine load increased. The growth rate in diffusive aggregation plays an important role in agglomerate growth. Increasing engine load leads to a decreasing growth rate. These decreasing growth rates can cause an increase in the size of soot agglomerates[20]. High pressure conditions (with the high engine load) produce increased drag on the agglomerates in the continuum region. Increasing drag strongly affects the rate of transport and thus collisions that lead to increasing agglomeration[21].

The fractal dimension (D_f) gives additional information on the mechanism of agglomerate growth shown in Table 2. This constancy of fractal dimension because of pilot injection quantities that the formations of this particulate agglomerate were governed by a diffusion mechanism. The average fractal dimension was determined by using low magnification images together with equations (1) and (2). The fractal dimension ranged from 1.47 to 1.77. These results are similar to previously measured values (1.46~1.7) for a 1.7 L light duty diesel engine[9]. This also suggests that more compact and chain-like agglomerates are produced in a light duty diesel engine. However, the present results are significantly different from previously measured values for heavy duty diesel particulates (1.8~1.88)[9]. The reason for this difference between light and heavy duty engines is partly the influence of the mean free path. When the mean free path is smaller than the cluster size, agglomerate growth is governed by the diffusion limit mechanism. Cluster and monomer particles are attached via Brownian motion for small mean free paths, thereby forming small chain-like agglomerates[22]. The data indicate that the difference in PM mass between low and high engine loads is strongly influenced by PM morphology factors, including the effect of primary particle size, agglomerate size (radius of gyration), number of agglomerates, and fractal dimension.

3.2. HC, CO and NOx, emissions

Fig. 7 shows the exhaust emissions of HC and CO. As shown in the figure, the HC emissions ranged from 7 ppm (at the 40% engine load) to 28 ppm (at the 0% engine load) for the two pilots/main injection. The HC emission is decreased 41% as the engine load increased from 0% to 40% with one pilot/main
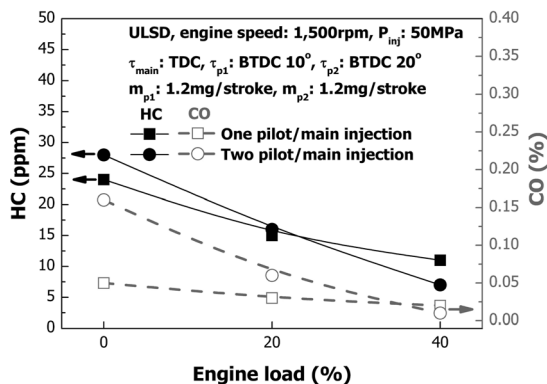

Fig. 6. Primary particle and agglomerate size as a function of engine load for the two injection strategies.

Fig. 7. Effect of the two injection strategies on CO and HC gas emissions for the three different engine loads.

injection. Similar behavior was observed with two pilots/main injection. CO ranged from 0.01% (at 0%) to 0.16% (at 40%) for the two pilots/main injection. The CO concentration decreased 40 % as the engine load was increased with two pilots/main injection. Similar behavior was observed with one pilot/main injection. The maximum CO emissions for the two pilots/main injection strategy was 0.16% (at 0%), while that for the one pilot/main injection strategy was 0.05% (also at 0%). The reduction of HC and CO may have been caused by increasing the injection mass with increasing engine load. In this case, CO and HC emissions according to engine load was similar trends as illustrated in Fig. 7.

Fig. 8 show the NOx for all three engine operating loads and two injection strategies. The NOx emissions ranged from 29 ppm at 0 Nm with one pilot/ main injection to 271 ppm at 40% load with two
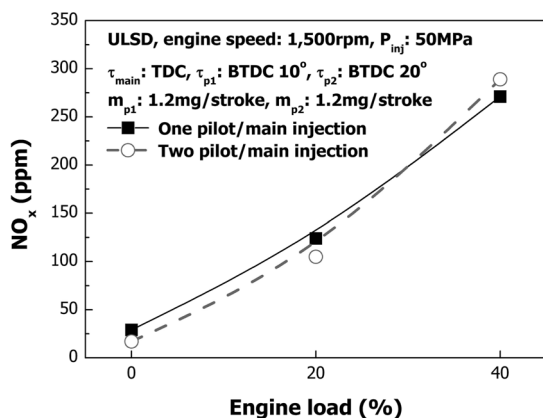

Fig. 8. Effect of the two injection strategies on NOx emissions for the three different engine loads.

pilots/main injection. As the engine load was increased from 0% to 40% with one pilot/main injection, the NOx emissions increased more than nine-fold as shown figure. Similar behavior was observed with two pilots/ main injection. NOx formation is strongly influenced by the stoichiometric air-fuel ratio, injection timing, and initial temperature of the charged air and combustion chamber. Previous research has reported that NOx formation is reduced as injection timing is delayed. However, the injection timing was not an important factor here since it was fixed[11]. The high engine load have led to increased initial temperatures which may have caused increased NOx formation. In addition, high engine loads make for a rich stoichiometric air-fuel ratio due to the increase in initial air consumption caused by the increased number of pilot injections and injection mass.

4. Conclusions

In order to investigate the effect of injection strategy and engine loads on the PM morphology and exhaust emissions, a thermophoretic sampling method with a scanning electron microscope (SEM) and opacity method of soot were applied to a four cylinder DI diesel engine. The conclusions can be summarized as follows:

The mass of the particulate matter (PM) increased in accordance with the increase of engine loads under the same operating conditions.

The PM morphology indicated that primary particle size and radius of gyration increased as engine loads were increased with both injection strategies.

The CO and HC emissions showed the similar decreasing trends according to two injection strategy.

When the engine load was increased from 0% to 40%, the mean size of the primary particles and the radius of the agglomerates increased. Also, the experimental fractal dimension increased from 1.32 at 0% of engine load to 1.43 at 40% of load with the one pilot/main injection strategy.

PM mass at low engine loads was three times higher than that of the 40% engine load with both injection strategies. The primary particle size, the agglomerate size, and the number of agglomerates were all strongly influenced by the mass of the particulate matter.

Acknowledgements

References

[1] Harris, S. J., Maricq, M. M., "Signature size distributions for diesel and gasoline engine exhaust particulate matter", Journal of Aerosol Science, Vol. 32, No. 6, 2001, 749-764

[2] Kennedy, I. M., "The health effects of combustion generated aerosols", Proc. Combust. Inst., Vol. 31, No. 2, 2007, 2757-2770

[3] U. S. Environmental Protection Agency, "Health assessment document for diesel", rept.2002, Washington DC, EPA/600/8-90/057F

[4] U. S. Department of Energy, "Annual Energy Outlook 2006 with projections to 2030", 2006, DOE/EIA-0383

[5] Tong, H. Y., Hung, W. T., Cheung. C. S., "On-Road Motor Vehicle Emissions and Fuel Consumption in Urban Driving Conditions", J. Air & Waste Manage. Assoc., Vol. 50, No. 4, 2000, 543-554

[6] Agarwal, A. K., "Biodiesel Development and Characterization for Use as a Fuel in Compression Ignition Engines", Transactions of the ASME, Vol. 123, No, 2, 2001, 440-447

[7] Flower W. L., Bowman, C. T., "Measurements of the Structure of Sooting Laminar Diffusion Flames at Elevated Pressures", Proc. Combust. Inst., Vol. 20, No. 1, 1984, 1035-1044

[8] Zhu, J., Lee, K., Panov, A., Akers J., Habeger, C., "An Investigation of Particulate Morphology, Microstructures, and Fractal Geometry for ael Diesel Engine-Simulating Combustor", SAE paper, 2004, 2004-01-3044

[9] Zhu, J., Lee, K. O., Yozgatligil, A., Choi, M. Y., "Effects of engine operating conditions on morphology, microstructure, and fractal geometry of light-duty diesel engine particulates", Proc. Combust. Inst., Vol. 30, No. 2, 2005, 2781-2789

[10] Neer, A., Koylu, U. O., "Effect of operating conditions on the size, morphology, and concentration of submicrometer particulates emitted from a diesel engine", Combust. Flame., Vol. 146, No. 1-2, 2006, 142-154

[11] Kim, M. Y., Yoon, S. H., Lee, C. S., "Impact of Split Injection Strategy on the Exhaust Emissions and Soot Particulates from a Compression Ignition Engine Fueled with Neat Biodiesel", Energy & Fuels, Vol. 22, No, 1, 2008, 1260-1265

[12] Musculus, M. P. B., "Measurements of the influence of Soot Radiation on In-Cylinder Temperatures and Exhaust NOx in a Heavy-Duty DI Diesel Engine", SAE Paper, 2005, 2005-01-0925

[13] Kim, M. Y., Yoon, S. H., Park, K. H., Lee, C. S., "Effect of Multiple Injection Strategies on the Emission Characteristics of Dimethyl Ether (DME)-Fueled Compression Ignition Engine", Energy & Fuels, Vol. 21, No. 5, 2007, 2673-2681

[14] Manzello, S. M., Choi, M. C., "Morphology of soot collected in microgravity droplet flames", International Journal of Heat and Mass Transfer, Vol. 45, No. 5, 2002, 1109-1116

[15] Chandler, M. F., Teng, Y., Koylu U. O., "Diesel engine particulate emissions: A comparison of mobility and microscopy size measurements", Proc. Combust. Inst., Vol. 31, No. 2, 2007, 2971-2979

[16] Hu, B., Yang, B., Koylu U. O., "Soot measurements at the axis of an ethylene/air non-premixed turbulent jet flame", Combust. Flame., Vol. 134, No. 1-2, 2003, 93-106

[17] Onischuk, A. A., Stasio, S. D., Karasev, V. V., Baklanov, A. M., Makhov, G. A., Vlasenko, A. L., Sadykova, A. R., Shipovalov, A. V., Panfilov, V. N., "Evolution of structure and charge of soot aggregates during and after formation in a propane/air diffusion flame", Journal of Aerosol Science, Vol. 34, No. 4, 2003, 383-403

[18] Böhm, H., Feldermann, C., Heidermann, T., Jander, H., Lüers, B., Wagner, H. G., Soot formation in premixed C2H4 - air flames for pressures up to 100bar Proc. Combust. Inst., Vol. 24, No. 1, 1992, 991-998

[19] Su, D. S., Müller, J. O., Jentoft, R. E., Rothe, D. Jacob, E., Schlögl, R., "Fullerene-Like Soot from Euro IV Diesel Engine: Consequences for Catalytic Automotive Pollution Control", Topics in Catalysis, Vol. 30-31, 2004, 241-245

[20] Witten, T. A., Sander, L. M., "Diffusion-limited

aggregation", Physical Review B, Vol. 27, No. 9, 1983, 5686-5697

[21] Matsoukas, T., Friedlander, S. K., "Dynamics of aerosol agglomerate formation", Journal of Colloid and Interface Science, Vol. 146, No. 2, 1991, 495-506

[22] Lee K. O., Cole, R., Sekar, R., Choi M. Y., Kang, J. S., Bae, C. S., Shin, H. D., "Morphological investigation of the microstructure, dimensions, and fractal geometry of diesel particulates", Proc. Combust. Inst., Vol. 29, No. 1, 2002, 647-653